

# **PEFORMANCE OPTIMIZATION OF INLINE SEPARATOR**

By

Ahmed Alawi Ahmed Alawadhi

15716

Dissertation submitted in partial  
fulfillment of the requirement for the

Bachelor of Engineering

(Hons) (Petroleum

Engineering)

May 2015

Supervisor: DR Shiferaw Regassa Jufar

Universiti Teknologi  
PETRONAS Bandar Seri  
Iskandar  
31750 Tronoh  
Perak Darul Ridzuan

# **CERTIFICATEION OF APPROVAL**

## **Performance Optimization Of Inline Separator.**

By

Ahmed Alawi Alawadhi  
15716

A project dissertation submitted to  
the Petroleum Engineering Programme  
Universiti Teknologi PETRONAS  
in partial fulfilment of the requirement for the  
BACHELOR OF ENGINEERING (Hons)  
(PETROLEUM)

Approved:

---

Dr Shiferaw Regassa Jufar

Approved:

---

Dr Narahari Marneni

UNIVERSITI TEKNOLOGI PETRONAS

TRONOH, PERAK

May 2015

## **CERTIFICATION OF ORIGINALITY**

This is to certify that I am responsible for the work submitted in this project, that the original work is my own except as specified in the references and acknowledgements, and that the original work contained herein have not been undertaken or done by unspecified sources or persons.

---

AHMED ALAWI AHMED ALAWADHI

## ABSTRACT

Inline Separator technology has been applied in a number of onshore and offshore wells to separate oil and water. The Benefits of using this technology include reduced produced water, as well as a significant reduction in cost of surface facilities. In addition, inline separator system is an environment friendly technology so it can be replace conventional separator. The intent of this project is to investigate and analyze the flow characteristics of the single phase in inline separator. Nine models with different inlet velocities and swirl angles were used to study the behavior of the flow in inline separator. For this purpose, computational fluid dynamics (CFD) Ansys –fluent is utilized to simulate these models. The radial distribution of the static pressure and axial velocity are also discussed. Multi objective optimization study of pressure drop in inline separator has been performed using CFD data and response surface methodology. Finally, the result has shown that the inlet velocity has more effect than swirl angle on the separation performance.

**Keywords:** Inline separator, swirl number, Computational Fluid Dynamic (CFD), pressure loss, flow patterns. Response surface methodology (RSM).Multi-objective optimization.

## **ACKNOWLEDGMENTS**

First and foremost, all praise is to Allah, the Most Gracious and the Most Merciful, Who through His mercy and grace, I was able to complete my final year project. Next I would like to express my appreciation to my Final Year project supervisor, DR Shiferaw Regassa Jufar, .He has been very dedicated to coach and is willing to share his knowledge value whenever I ask him questions regarding to the project .I could have not completed this project alone with the kind help and his guidance from the very beginning. Also, I like to express my appreciation to my final year Project CO-supervisor DR Tamiro Alemu for his endless support. He has provided me with all the necessary data and resources that helped me to enlarge my knowledge and experience in all project related aspects. My ultimate gratitude to him for his guidance, monitoring throughout my project. My deepest heart gratitude is to my parents who strived to get me where I'm now. Their spirit has guided me through my difficult times. Deep appreciation goes to my brothers and sisters. I dedicate this project to them and I highly appreciate their motivation and encouragement and their valuable advices that they provided me through all this period. Not to forget, I would like to Thank Universiti Teknologi PETRONAS (UTP) for their support and for providing me with the necessary equipment and software that was required to run the project smoothly.

## Table of Contents

CERTIFICATEION OF APPROVAL.....	li
CERTIFICATION OF ORIGINALITY.....	iii
ABSTRACT .....	iv
ACKNOWLEDGMENTS .....	v
Table Of Contents .....	vi
list Of Figures .....	viii
list Of Tables .....	ix
CHAPTER 1 .....	1
1.0 INTRODUCTION.....	1
1.1 Background .....	1
1.1 Problem Statement .....	3
1.2 Objectives .....	3
1.3 Scope of the study:.....	3
CHAPTER 2 .....	4
2.0 LITERATURE REVIEW .....	4
2.1 Inline separator design .....	4
2.2 inline separators technology .....	5
2.3 Swirling Flow.....	7
2.4.1 Navier-stokes Equation .....	8
2.4.1.1 Conversation of mass: .....	8
2.4.1.2 Momentum equation: .....	8
2.5 velocity field within inline separator.....	9
2.6 Response surface methodology (RSM) .....	9
CHAPTER 3 .....	10
3.0 METHODOLOGY .....	10
3.1 Research methodology.....	10
3.2 Research Methodology Procedure .....	10
3.3Computational Fluid Dynamics (CFD) ANSYS-FLUENT.....	11
3.4 Work Process Flow of simulation (using Ansys ,CFD-FLUENT): .....	12
3.4.1 Define Geometry model and Meshing: .....	12
3.4.3 Setup: .....	13
3.4.4 Solution:.....	14
3.4.5 Result:.....	15

3.5 Project Key Millstone .....	16
3.6 Gantt chart: .....	17
CHAPTER 4 .....	18
4.0 RESULTS AND DISCUSSION .....	18
4.1 Parametric studies .....	18
4.2 Radial distribution of the static pressure .....	20
4.3 Multi-objective optimization using response surface methodology .....	22
4.3.1 Fitting the model:.....	22
4.3.2 Analysis of response surface plots .....	24
4.3.3 Multiple Response Optimization.....	26
CHAPTER 5 .....	28
5.0 CONCLUSION AND RECOMMENDATION .....	28
REFERENCES .....	29
Appendixes .....	31

## LIST OF FIGURES

Figure 1: Example of tangential and axial cyclones .....	2
Figure 2: schematic design of inline separator .....	4
Figure 3: The inline Desander .....	5
Figure 4: The inline Dewater .....	6
Figure 5: The inline DeLiquidizer .....	6
Figure 6: Jet flow with low degree of swirl .....	7
Figure 7: Jet flow with high degree of swirl.....	7
Figure 8: Project workflow chart.....	10
Figure 9: simulation procedure.....	11
Figure 10: work process of simulation.....	12
Figure 11: Mesh on the surface of ISE.....	12
Figure 12: viscous model setup .....	14
Figure 13: solution method .....	14
Figure 14: project keymilstone.....	16
Figure 15: wall static pressure along the pipe axis .....	29
Figure 16: static pressure along the axis of the pipe .....	20
Figure 17: Radial distribution of the static pressure .....	21
Figure 18: Radial distribution of axial velocity .....	21
Figure 20: 3D scatter plot.....	24
Figure 22: 3D surface plot .....	25
Figure 23: 2D contour plot of pressure rop .....	25
Figure 19: Main effect plot .....	25
Figure 21: Pareto chart.....	26



## LIST OF TABLES

Table 1 Boundary conditions-----	13
Table 2 Ganttchart for FYP1 -----	17
Table 3 Ganttchart for Fyp2 -----	17
Table 4 Parametric studies-----	18
Table 5 Regression Analysis -----	23
Table 6 Analysis of variance -----	23
Table 6Multiple response optimization -----	27
Table 7 Optimization input parameter -----	27

# **CHAPTER 1**

## **1.0 INTRODUCTION**

### **1.1 Background**

Recently, Produced water is one of the largest issues in oil and gas industries. The oil stream contain high amount of water which is range between 75-95 % water in some offshore and onshore oilfields [1]. American Petroleum Institute (API) reported that about 20 billion barrels of produced water were produced by U.S onshore oilfields operations in 2002[2].Also, large volume of water are produced from thousand of wells in different countries. Increasing the amount of Produced water lead to increase the cost in managing the increase volume of produced water to lift to the surface, also produced water treatment is required more space for facilities in the platform and it is enormously cost[3]. Therefore, the efficient separation of oil from water becomes an increasingly important processing step. This separation of the phases is required in order to reduce the demands on the transport facilities and to facilitate re-injecting the separated water into reservoir to maintain the well pressure.

Generally, separation can be achieved by using the action of gravity in very large vessels .But, large costing is needed since large weight and space requirements for on-site processing favorite [4]. However, the on-date research suggested much smaller and cheaper alternative by using in-line separator that used swirling flow to separate the phases .the driving force behind separation of the phases in inline separator is the centrifugal force which can be a hundred times larger than gravity[5] .Swirling flow has been used successfully for separation of solid from either liquid[6] or gas[7]. Liquid-liquid separation presents more challenges due to poor coalescence, high volume fractions of dispersed phase, the smaller density differences, and danger of emulsion formation. In fact, smaller size reduces hydrocarbon that lowers the safety risk subsequently making lower costs for maintenance and inspection using piping compared to vessels[8].

As shown in figure (1) there are different methods to create a swirling flow in a cyclone. The conventional ways are tangential inlets as used in tangential hydrocyclone. The flow in this type enters tangentially into a hydrocyclone and this creates a strong rotation. The cyclones developed until now for deoiling water and dewatering oil are based on this design (Dirgo and Leith,1986). The another type of cyclone is also shown in figure 1, the axial cyclone in the form of a cylindrical pipe.. This type uses vanes to produce swirl flowing. The main advantages of an axial cyclone over a tangential cyclone are: less pressure drop, more compact design, and less turbulence.(Swanborn,1988).

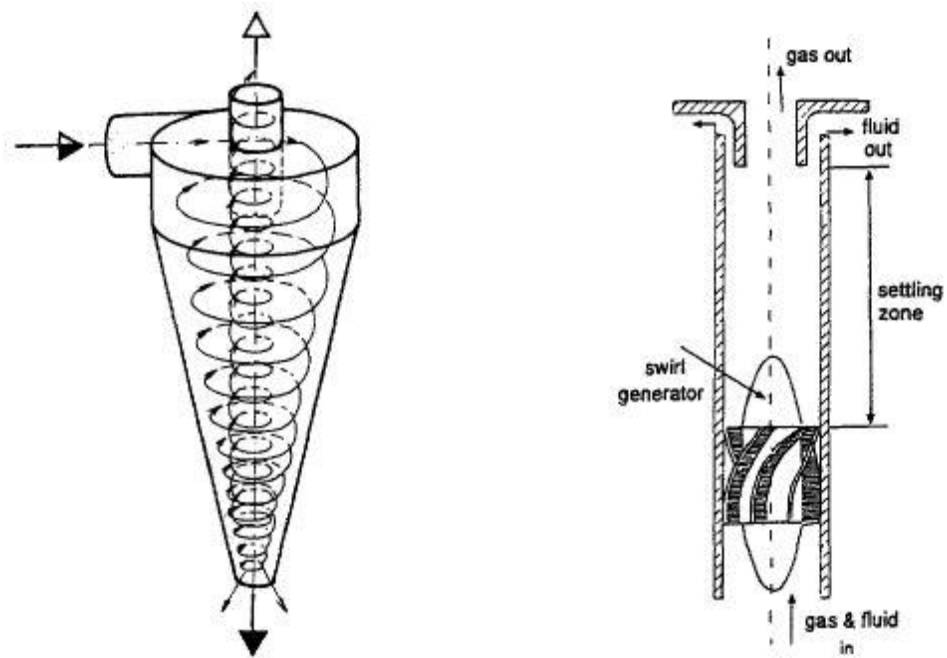


Figure 1 Examples of tangential cyclone(left) and axial cyclone(right)[9]

Although the separator will be used for multi-phases flow in axial cyclone, it is important to analyze single phase-flow first because it is less complex, and computationally less expensive than multiphase flow. Thus, it is easier to study the single phase flow behavior in parameter studies. On top of that, single-phase flow is easier understood making it higher accuracy and producing reliable results when It is modeled. Therefore, in this project only the single phase flow characteristics in inline separator is investigated.

## **1.2 Problem Statement**

Due to wide applications of cyclone separator in oil industries, there are many studies to optimize the performance of the separator. However, these studies are limited only on the gravity separator. From the above limitations, more investigate and studies are needed on inline separator to understand the behavior of single phase flow and to know the effect of the swirling angle and inlet velocity on the separation performance.

## **1.3 Objectives**

The main objectives of this project are:-

- To investigate the flow characteristics of a swirling flow in a single phase inline separator.
- To predict the pressure drop inside the inline separator.
- To optimize the performance of Inline separator.

## **1.4 Scope of the study:**

The boundaries of this project are to study the flow behavior of single phase flow in inline separator and to optimize the performance of the separation. Assuming steady state conditions, nine numerical models of inline separator will be designed using Computational Fluid Dynamics (CFD) ANSYS 15.0 workbench and flow equations solved using CFD-Fluent solver.

## CHAPTER 2

### 2.0 LITERATURE REVIEW

#### 2.1 Inline separator design

The prototype design of inline separator is based on Delfos prototype designed as shown in figure(2) [9] .It consists of stationary internal swirl element (ISE) placed in a pipe of 100 mm internal diameter. This ISE is made of a central body which is equipped with 9 vanes attached to the wall of the pipe and to surface of the central body .The pick-up tube is placed 1.7 m downstream of the ISE .it is straight pipe with an outer diameter of 50 mm and wall thickness of 1 mm.

The typical inline separators have performed the same function as the conventional separators, but in the conventional separation of two phases are achieved under the influence of gravity after the fluids have long retention time. While with inline separator, the speed of separation is increased, so the need for long retention time within inline separator eliminated..As the incoming flow is accelerated towards the narrow vane section, the fluid is deflected, thus generating swirling flow [10]. The separation in inline separator can be achieved by using the centrifugal force resulting in flow patterns to separate fluid phases (Al-Qahtani, &Boud,2008) .Principally, higher axial velocity and relatively large radius at which vanes are placed increases the angular momentum. Meanwhile, at downstream of ISE, strongly swirling flow combined with centrifugal forces up to 300g will force the lighter oil phase into center of pipe where is then collected at a further downstream by a pickup tube[11].

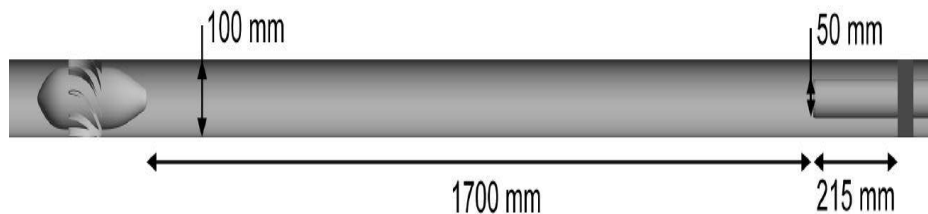


Figure 2 schematic design of inline separator (Delfos model designed)

## 2.2 inline separators technology

The inline separation technology has attracted the attention of petroleum field operators because inline separator has many advantages compared to the conventional separators.. Compact separation solutions have established substantial attention for offshore production technology over many years (Westra ,DeHaas,&Fantoft,2010). For instant, the implementation of inline separator system called 'Flow Induced Inline Separation' (FIIS) is used at the Gullfakes Field. FIIS consists of four units which are DE-Sander,De-watering Unit, Phase-Splitter and De-Liquidizer.The separation process for all these FIIS units is by using an internal swirl element (ISE) and vanes to force the multiphase flow and deflect the flow of the fluid, therefore utilizing centrifugal force to separate two phases of different densities (Eidsom & Bjorkhanug,).

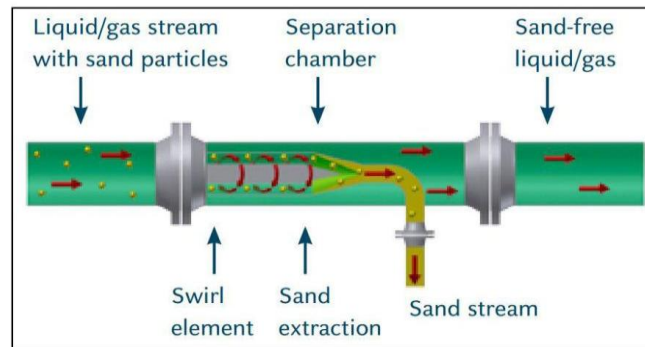


Figure 3 The inline Desander

The inline Desander as shown in figure (3) can be used to remove sand from single and multiphase fluids as it might be customized to suit any application. It can handle a wide range of flow rates and achieve efficiency up to 99% due to its compact cyclonic unit without any reject streams. Up to 1 micron of particle sizes can be removed depending on the size of the unit .(FMS Technologies).

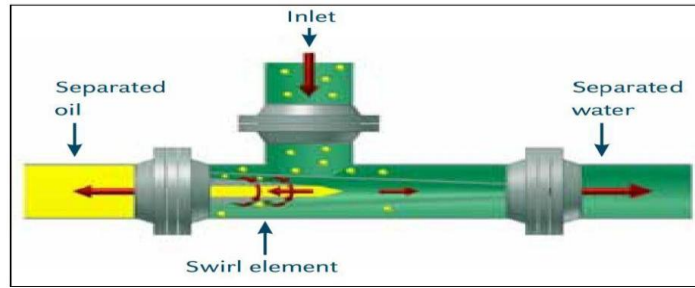


Figure 4 The Inline DeWatar

As shown in figure(4) the Inline DeWatar is an axial flow cyclone that uses a fix internal swirl element. Also It is a compact cyclonic unit designed for efficient separation of two phases which combines high efficiency with low pressure drop in a compact design. This inline separator has been qualified and developed with Statoil company and during testing they found that efficiencies exceeding 99%.(FMC Technologies,2011).

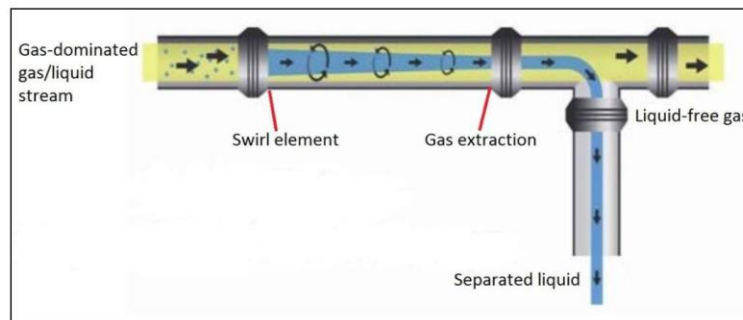


Figure 5 The inline DeLiquidizer

An inline DeLiquidizer in figure (5) used to improve the overall gas scrubbing efficiency by removing liquid from gas upstream on existing scrubber. It was developed and applied at Statoil Sleipner field. A liquid film forms on the wall of the equipment as the liquid stream containing gas entered the internal swirl element. (FMS Technologies).

### 2.3 Swirling Flow

Swirling flows are found in nature and occur in wide range of applications. For example, inline separators, hydrocyclone separators, heat exchanger, vortex amplifiers, and many other practical devices [12]. Generally, there are three methods to generate swirling flow, direct tangential entry, swirl vane and rotation of the pipe [13]. Many researches and studies show that swirl flow has large effect on the cyclone flow field. This flow field can be characterized by a swirl number, which is a non-dimensional number [14]. Swirl number can be defined as the angular momentum flux divided by the momentum flux times the pipe radius (Kito, 1984)

Gupta, Lilley, and Syred (1985) reported that the effects of the inlet flow swirl on the flowfield produced are increasingly dramatic as the swirl number increases. They observed that jet flow with low degree of swirl (weak swirl  $<0.4$ ) resulting in large lateral pressure gradients only and a wider slower jet than its nonswirling counterpart as shown in figure (6). When the jet flow with high degree of swirl (strong swirl  $>0.6$ ) as shown in figure (7) resulting in large longitudinal and lateral pressure gradient, a much wider, slower jet than its nonswirling counterpart [15].

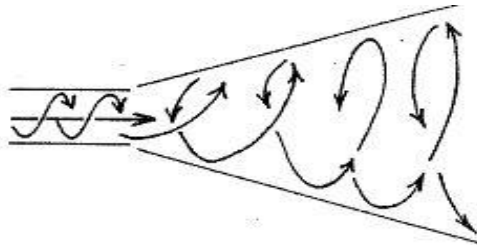


Figure 6 Jet flow with low degree of swirl [12]

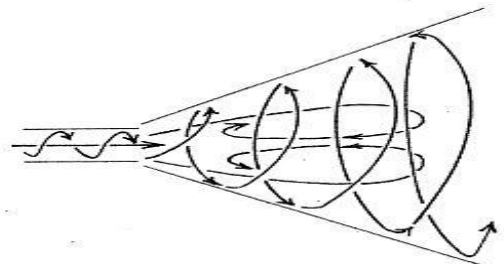


Figure 7 Jet flow with high swirl [12]



## 2.4 Governing equation:

### 2.4.1 Navier-stokes Equation

The steady flow of an incompressible liquid is generally solved using the Navier-stokes equation (blasek, 2005). To describe the physical properties of the fluid mathematically Navier-stoke equation is used by applying the conservation law of the physical properties of fluid such as ,conservation of mass, conversation of momentum and conservation of energy .

#### 2.4.1.1 Conversation of mass:

Mass conservation is the physical of continuity equation, assuming isothermal flow condition where the rate at which mass entering the system is equal to the rate at which mass leaves the system. The continuity equations for water and oil phase, can be expressed as :

$$\frac{\partial \rho_w}{\partial t} + \nabla \cdot (\rho_w \mathbf{v}_w) = 0 \quad [2.1]$$

$$\frac{\partial \rho_o}{\partial t} + \nabla \cdot (\rho_o \mathbf{v}_o) = 0 \quad [2.2]$$

For water phase (w) and oil phase (o),  $\rho$  is the density and  $\mathbf{v}$  is the velocity for both phases .the mass rate increase in time is represented by the first term of the equation where the second term of the equation represents the mass flow out of the control volume. The total volume fraction for both phases is equal 1

$$k_w + k_o = 1 \quad [2.3]$$

At steady state condition;  $\frac{\partial \rho}{\partial t} = 0$

#### 2.4.1.2 Momentum equation:

Momentum equation models the interaction between each phase, it involves that forces acting on each phase and interphase momentum. The equation for water phase is as described below:

$$\rho_w k_w \left[ \frac{\partial \mathbf{v}}{\partial t} + \mathbf{v}_w \cdot \nabla \mathbf{v}_w \right] = -k_w \nabla P + k_w \nabla \tau_w + \rho_w k_w \mathbf{g} - \mathbf{M} \quad [2.4]$$

Correspondingly, for oil phase

$$\rho_o k_o \left[ \frac{\partial \mathbf{v}}{\partial t} + \mathbf{v}_o \cdot \nabla \mathbf{v}_o \right] = -k_o \nabla P + k_o \nabla \tau_o + \rho_o k_o \mathbf{g} - \mathbf{M} \quad [2.5]$$

At steady state condition;  $\frac{\partial \rho}{\partial t} = 0$

## 2.5 velocity field within inline separator

The separation of the fluid can be affected by the velocity field in the inline separator [16]. The mean velocity distributions were described by Kitoh (1991). The radial velocity distribution is determined from the continuity equation using the measured mean axial velocity. The tangential velocity distribution enables a division of the flow in three regions: the wall region, core region and annular region. The wall region is dominated by steep gradients. The annular region is characterized by a free vortex behavior and the core region is characterized by a forced vortex type velocity distribution. The axial velocity can be predicted by using a third-order polynomial equation [17]. Tangential velocity has been confirmed to be consisting of a combination of a free-like vortex in the outer wall region and a forced vortex near the inline separator axis.

## 2.6 Response surface methodology (RSM)

RSM is a powerful statistical analysis method which has been employed in the field of Engineering and manufacturing [18]. RSM method was introduced by Box and Wilson in 1951 [19]. Today RSM is the most generally used method of process optimization. According to Carter and Myers (1989) the important development of optimal design theory in the field of experimental design emerged following World War II. In order to conduct an RSM analysis, identify the experiment parameters to adjust, and define the process response to be optimized. In general, the response surface can be visualized graphically. The graph is helpful to see the response surface; valleys, ridge lines and hills. The second-order polynomial model used in the response surface analysis has the form:

$$Y = \beta_0 + \sum_{i=1}^7 \beta_i X_i + \sum_{i=1}^7 \beta_{ii} X_i^2 + \sum_{i < j} \sum \beta_{ij} X_i X_j$$

Where  $\beta_0, \beta_i, \beta_{ii}$ , and  $\beta_{ij}$  are the regression coefficients for intercept, linear, quadratic and interaction terms, respectively. While  $X_i$  and  $X_j$  are the independent variables and  $Y$  is the response variable (pressure drop).

## CHAPTER 3

### 3.0 METHODOLOGY

#### 3.1 Research methodology

Methodology is the process that describes techniques and materials that applied to field of study to collect important data. This chapter covers the process and methods undertaken through the project to achieve the objectives of this study.

#### 3.2 Research Methodology Procedure

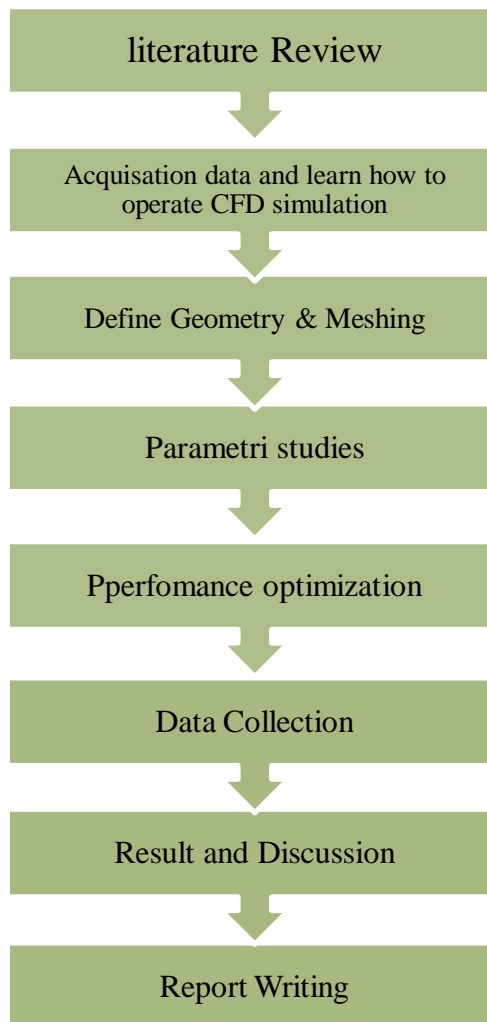


Figure 8 project workflow chart

### 3.3 Computational Fluid Dynamics (CFD) ANSYS-FLUENT

Computation Fluid Dynamics (CFD) software is one of the strongest engineering software that is generally used in various engineering sectors such as chemical, civil, mechanical, petroleum, aeronautical and astronautical engineering to set up simulation. The first CFD investigation study in the flow field of cyclone separator was by Boysan et al.1983 [20]. From that time, CFD method is widely used to obtain pressure drop across cyclone separator and predict the characteristics of cyclone field flow in details. For example, Jolius and T.G. Chuah (2004) computationally investigated the effects of inlet velocity and temperature on the pressure drop of the gas cyclone separator. They observed that CFD simulations predicted perfectly pressure drop of the cyclone separator with only deviation of 3 % from the measured. In this project, prediction of pressure losses of inline separator will be performed using ANSYS 15.0 CFD-FLUENT. Turbulent  $k - \epsilon$  model.

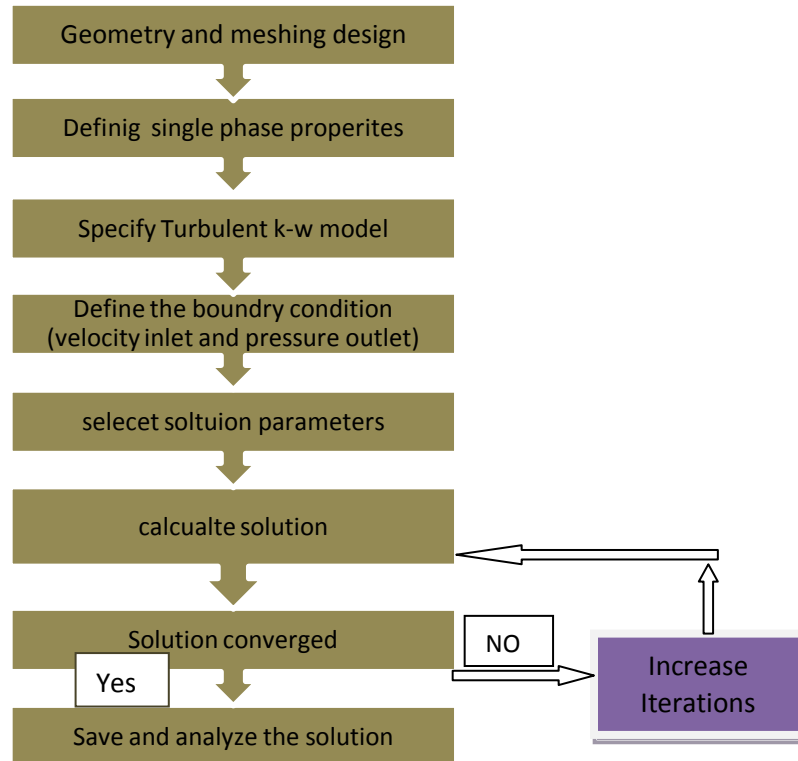


Figure 9 Simulation Procedure

### 3.4 Work Process Flow of simulation (using Ansys ,CFD-FLUENT):

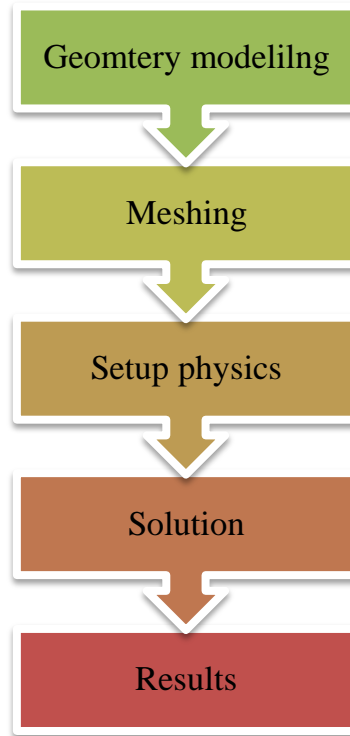


Figure 10 Work process of simulation

#### 3.4.1 Define Geometry model and Meshing

Geometry modeling is the first step of simulation process. All geometry models were constructed according to the exact dimensions of Delfos model as shown in figure 2. All geometrical designs were made in three dimensional (3D) because it is an easy method of constructing and to reduce the computation cost. After construct the geometry model , the next step is meshing as shown in figure 11. The importance of the meshing is as certain the accuracy of obtained results and influence the speed of the solution. the governing factors of good mesh includes size of mesh, shape of mesh used, uniformity of mesh geometry etc. Smaller size of mesh would give more detailed simulation results with give extra time.

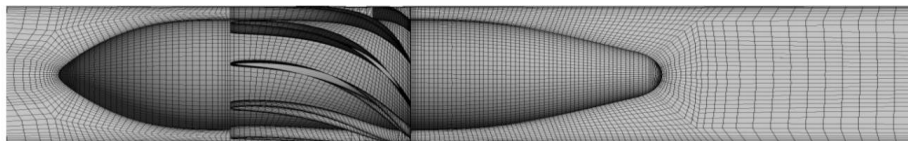


Figure 11 Mesh on the surface of ISE and on the plane through the axis on the separator .1.4 M hexahedral element are used for mesh [18]

### 3.4.3 Setup

After completing the meshing, the geometry model is then run in Ansys Fluent 15. at this stage, specific settings such as model, materials, cell zone condition, boundary conditions are set for the model. The flowing setups were opted:

Solver type: pressure –based, as pressure is true unknown in all fluid flow computations regardless of compressible or else. Thus, pressure –based algorithms are valid .

Boundary condition: In fluent the cylinder walls and cell surface are treated as non-slip boundaries with standard wall function. Assuming the isothermal and steady state , the boundary conditions and physical parameters of oil-water mixture are shown in table 1 and table 3, respectively .

Boundary	Fluent boundary type
Inlet	Velocity inlet
Outlet	Pressure outlet
Wall condition	No -slip

Table (1) boundary conditions

Next, for models, turbulent viscous model is selected with option of k-epsilon is chosen as shown in figure (12). Typically, Reynold stress model used in calculation of high swirling flows. This model also requires high computational power and time consuming in competing simulations. Lately the k-epsilon model have been proven to yield similar results especially involving shear stress tension ,yet consuming less computational power and time compared to RSM. Standard k-epsilon model solves for kinetic energy k and turbulent frequency .This model performs better under adverse pressure gradient conditions, functional for complex boundary layer flow, and for a more accurate near wall treatment.

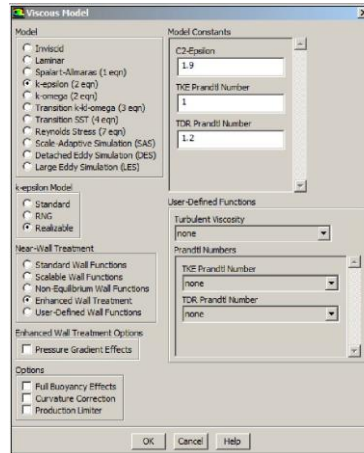


Figure 12 viscous model setup

### 3.4.4 Solution

The solution method selected is “SIMPLE” as it is a practical procedure used to solve Navier-Stokes equations. Second Order Implicit option for transient formulation is chosen. This is a common and advised practice to achieve better accuracy in the results of the simulation.

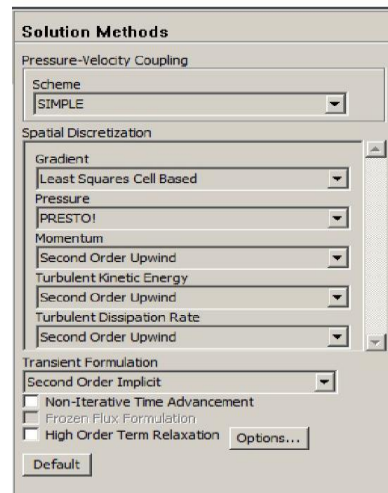


Figure 13 solution methods

### **3.4.5 Result**

As for results, the visual component used is CFD –POST which is bundled up together in the Ansys software package .Here, streamlines, contours, vector, etc might be produced to show clearly the results of simulation for further analysis. Moreover, it can be chosen to show contours or vectors only on surface e.g, a plane, rather than the whole volume of geometry .As per this simulation contour chosen to display results shown on bisecting planes. Alternatively graphs or charts can be opted to display the results.



### 3.5 Project Key Millstone

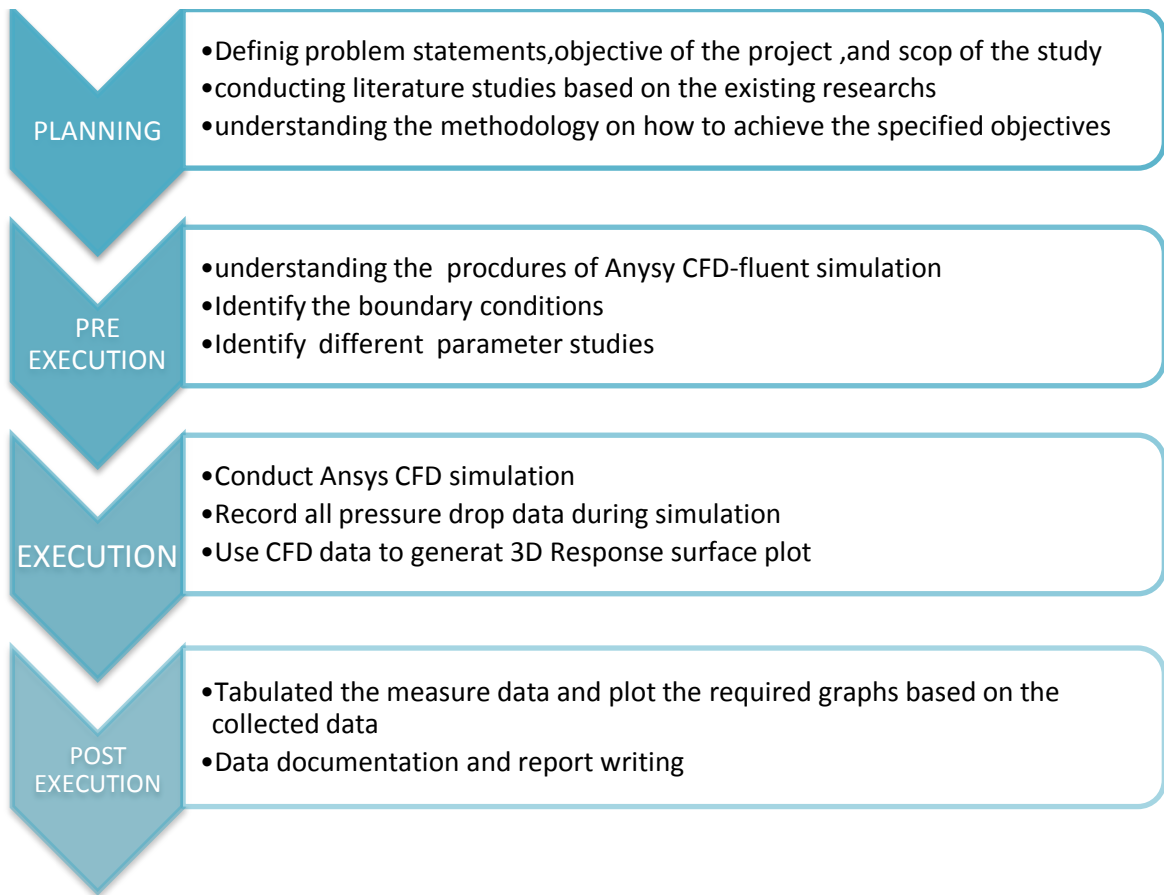


Figure 14 Project Key Millstone

### 3.6 Gantt chart:

Item / Week	1	2	3	4	5	6	7	8	9	10	11	12	13	14
Topics Selection														
Preliminary research work														
Extended proposal														
Proposal Defense Presentation														
Project Work Continues														
Interim Report draft submission														
Interim Report Submission														

**Table 2 Gantt chart for Final Year Project1 (FYP1)**

Item / Week	1	2	3	4	5	6	7	8	9	10	11	12	13	14	15
Developing MATLAB code and simulation work															
Progress report submission															
Simulation work continue															
Poster presentation (Pre - EDX)															
Dissertation draft submission															
Submission of dissertation (soft copy)															
Submission of Technical Paper															
Final oral presentation (Viva)															
Submission of project dissertation (hard bound)															

**Table 3 Gantt chart for Final Year Project 2 (FYP2)**

Legend	
Deadline	
Progress	

## CHAPTER 4

### 4.0 RESULTS AND DISCUSSION

In this section, steady state simulation results of velocity and pressure distribution of the flow behavior are discussed and analyzed. As shown from table (4). Nine models with variation of swirl angles and inlet velocities are investigated by using Ansys CFD-FLUENT.

#### 4.1 Parametric studies

Model	swirl angle	$\cos\theta$	$\sin\theta$	inlet velocity'm/s'	Pressure drop'Pa'
1	39.17	0.775312057	0.631578351	1.25	246
2	64.17	0.43575481	0.900065412	2.25	649.9
3	14.17	0.9695879	0.244743344	0.75	67.7
4	55.83	0.561602107	0.827407441	2.75	1340
5	22.5	0.923879533	0.382683432	4.25	2940
6	80.83	0.159306868	0.987229113	1.75	224
7	47.5	0.675590208	0.737277337	4.75	4520
8	72.5	0.3007058	0.953716951	3.75	1770
9	30.83	0.858661857	0.512542501	3.25	1876

Table 4 Parametric studies

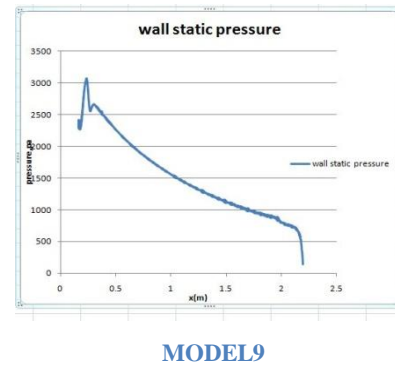
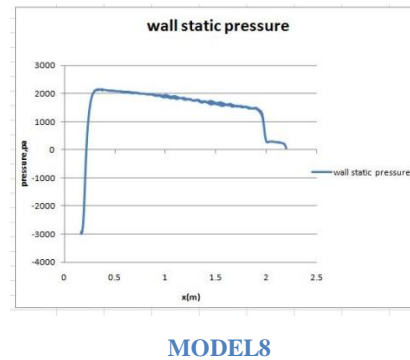
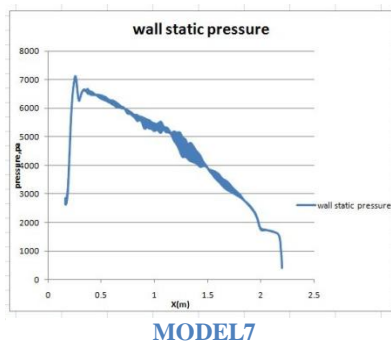
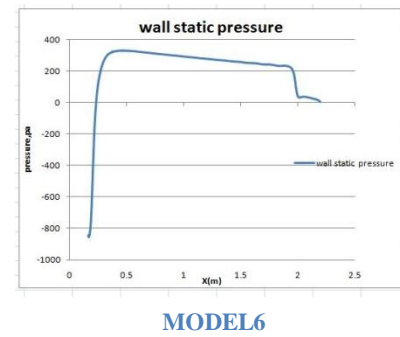
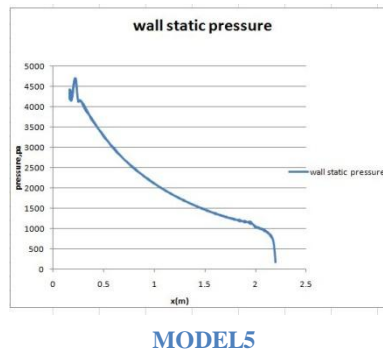
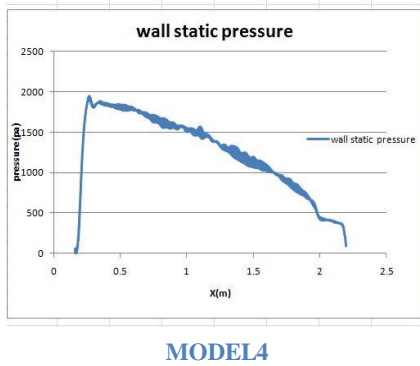
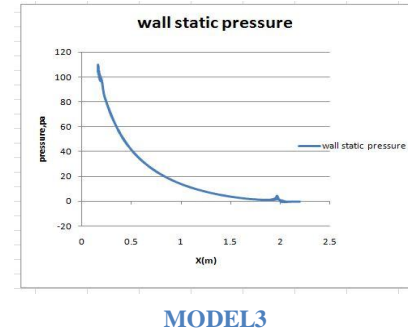
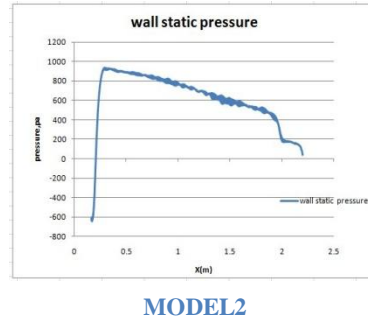
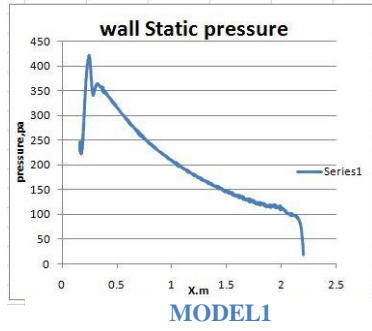


Figure 15 wall static pressure along the pipe line axis of inline separator

The static wall pressure along the pipe axis for the nine models is shown in figure (15). It can be seen that when the inlet velocity is high as in model 5 and 7 the wall static pressure at the internal swirl element is also high then it decreases rapidly at the downstream of internal swirl element as the flow face friction of boundary layers along the pipe axis. Also it can be noted that in model 4 compared with model 7 and model 6 compared with model 8. Although the inlet velocities are different, the pressure behavior is similar when the swirl angle is quite the same for all models which indicates the

effect of the swirl angle .it also observed that a negative pressure appears in the force vortex region for models 2,6 and 8 indicate the high swirling flow. in addition, for all the models the wall static pressure at the tail of the internal swirl element is lower compared with the pressure at the exist of the inline separator section.

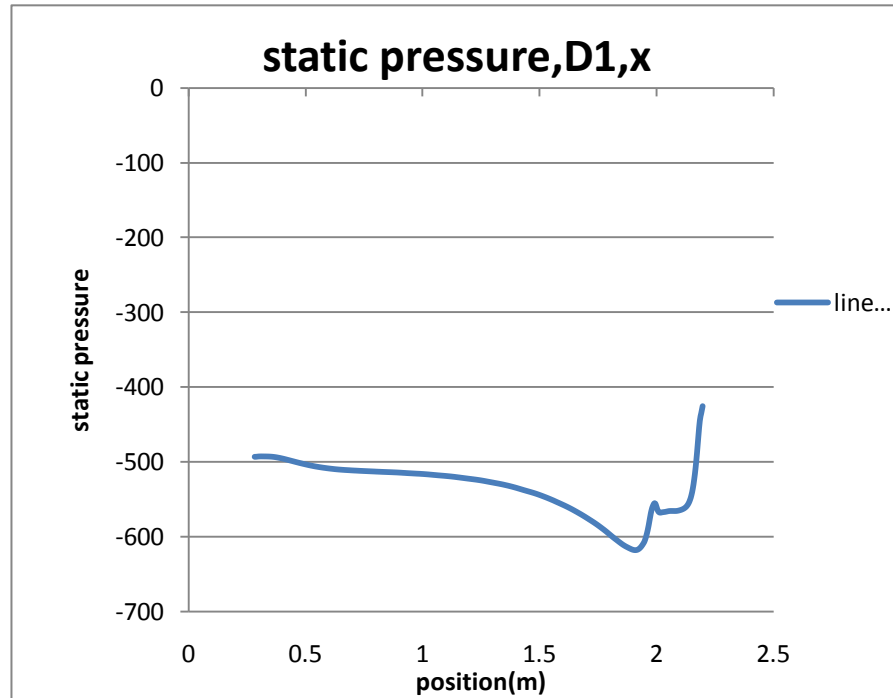


Figure16 static pressure along the axis of the pipe

From the graph as shown in the figure (16)above, it shows the radial distribution of static pressure along a line on the pipe wall, when inlet velocity is 1.25 m/s ,the static pressure decrease downstream of the ISE. The pressure increase at  $x=1.7$  m caused by presence of pick-up tube entrance.

## 4.2 Radial distribution of the static pressure

The profiles of the measurement for radial distribution of static pressure and axial velocity are shown for model 1 for the rest models the data graphs are shown in Appendix as the fact that radial distribution of static pressure and axial velocity show only minor differences with the data present in this chapter.

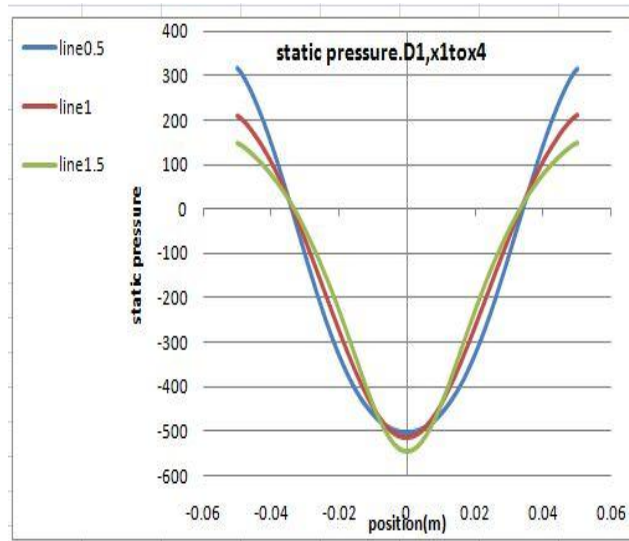


Figure 17 Radial distribution of the static pressure on the line through center of pipe at  $x=0.5, 1.0, 1.5$ .

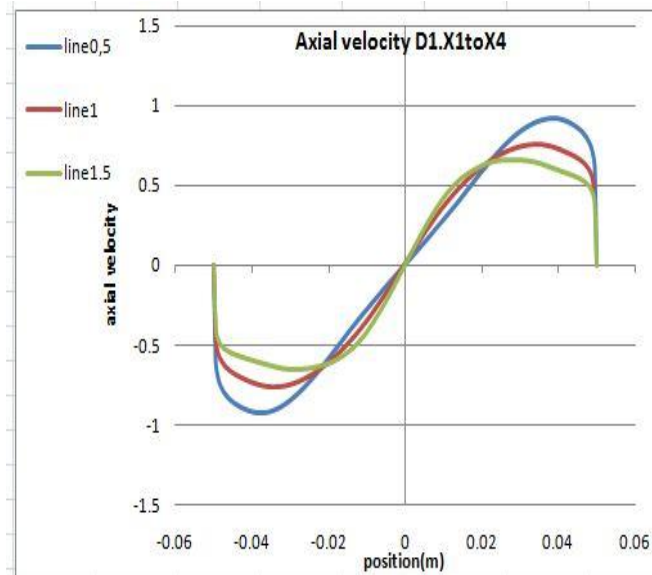


Figure 18 Radial distribution of the axial velocity on the line through center of pipe at  $x=0.5, 1.0, 1.5$ .

More detailed view of the flow characteristics can be obtained by examining the radial distribution of the static pressure and axial velocity on a line through the center of the pipe as shown in figure 17 and figure 18, respectively.

From the radial distribution in figure 17 it can be showed that the static pressure changes signs three times from the center to the wall of the pipe. The radial distribution of the axial velocity as shown in figure 18 can be match with radial distribution of static pressure. The negative static pressure near the wall, correspond with a positive axial velocity. In the very center the static pressure is also positive. It is also observed that when the static pressure increase the axial velocity start to decrease as shown in figure 17 and figure 18.

### **4.3 Multi-objective optimization using response surface methodology**

#### **4.3.1 Fitting the model:**

Analysis of variance (ANOVA) and regression analysis are used to examine fitted model to provide an adequate approximation of the true response surface. it can be observed from the table 6 large F-value (small P value ) would indicate a more significant effective on the respective response variable. Based on the results presented in table 6 and table 7 the variable with large effect on the pressure drop was inlet velocity since P-value less than one.

### 4.3.2 Regression Analysis

Regression coeffs. for Pressure Drop

<i>Coefficient</i>	<i>Estimate</i>
constant	-339.777
A:Inlet Velocity	-684.358
B:Swirl Angle	54.7881
AA	316.857
AB	-3.01257
BB	-0.511576

Table 5 Regression analysis

The regression equation for quadratic fit is:

$$\text{Pressure Drop} = -339.777 - 684.358*A + 54.7881*B + 316.857*A^2 - 3.01257*AB - 0.511576*B^2$$

Where A=Inlet Velocity

B=Swirl Angle

R-squared = **91.1451%**

R-squared (adjusted for d.f.) = **88.1935%**

Standard Error of Est. = **506.844**

Mean absolute error = **321.322**

Durbin-Watson statistic = **2.18992 (P=0.7650)**

### 4.3.3 Analysis of Variance

<i>Source</i>	<i>Sum of Squares</i>	<i>Df</i>	<i>Mean Square</i>	<i>F-Ratio</i>	<i>P-Value</i>
Model	1.58654E7	2	7.9327E6	30.88	<b>0.0007</b>
Residual	1.54134E6	6	256891.		
Total (Corr.)	1.74067E7	8			

Table 6 Analysis of Variance(ANOVA)

It can be shown from table 5, the results of fitting a multiple linear regression model to describe the relationship between pressure drop and two independent variables. It can be observed in table 6 when P-value less than 1, there is statistically significant relationship between the variables at 90 % confident level. The R-Squared statistic indicates that the model as fitted explains 91.1451% of the variability in pressure drop. The adjusted The adjusted R-squared statistic, which is more suitable for comparing models with different numbers of independent variables, is 88.1935%. The standard error of the estimate shows the standard deviation of the residuals to be 506.844. The mean absolute error



(MAE) of 321.322 is the average value of the residuals. The Durbin-Watson (DW) statistic tests the residuals to determine if there is any significant correlation based on the order in which they occur in your data file. Since the P-value is greater than 1, there is no indication of serial autocorrelation in the residuals at the 90.0% Confidence level.

#### 4.3.4 Analysis of response surface plots

For the visualization of the results Pareto chart , main effect plot, and response surface plots were created by using Statgraphics software. Based on the data in 3D scatter plot as shown in figure(21), the 3D surface plot can be generated by varying the inlet velocity and swirl angle that are taken from table 4. From the plot, pressure drop forms a plane within the independent factors .The corresponding 2-D contour plot of pressure drop regarding to these two factors is shown in figure (23). From the above figures it can be observed that how changes of swirl angle and inlet velocity affect the pressure drop. The lower of the inlet velocity and swirl angle the lower the pressure drop as shown in figure (22).

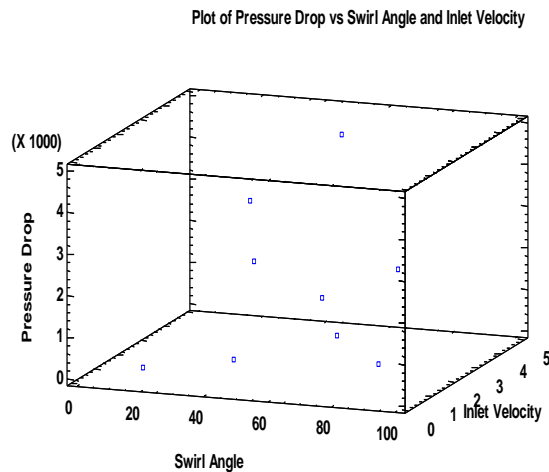


Figure 19 3D scatter plot

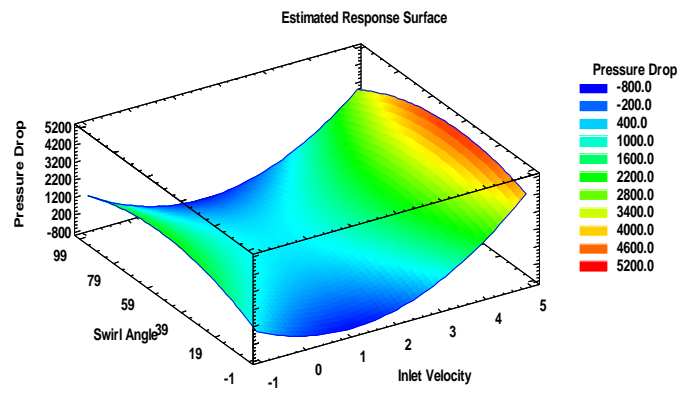


Figure 20 3D surface plot

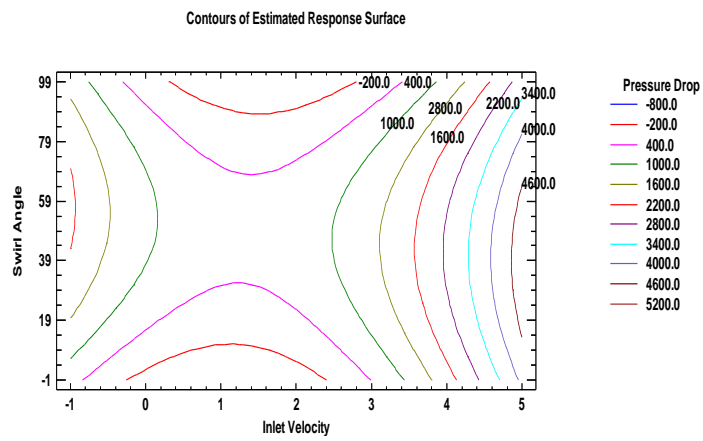


Figure 21 2D contour plot

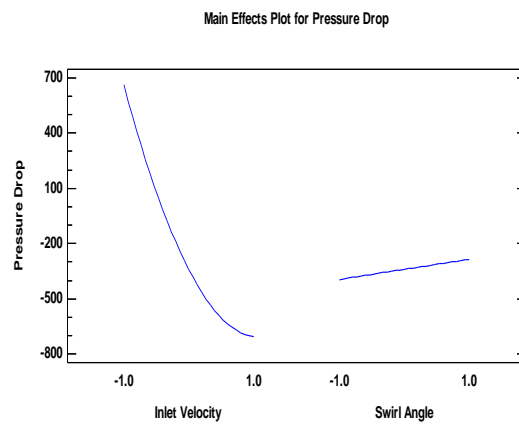


Figure 22 Main effect plot

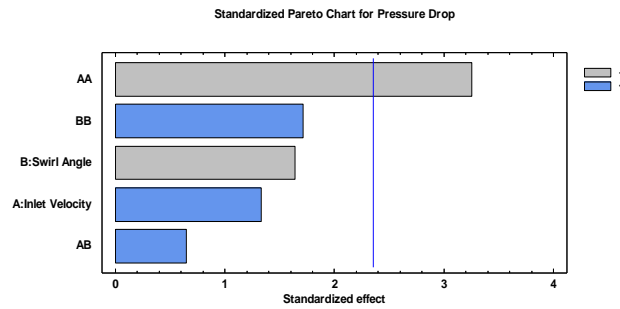


Figure 23 Pareto chart

Based on the main effect plot and the Pareto chart shown in figure 19 and figure 20, respectively, the most significant factor on the pressure drop is inlet velocity. Pareto chart displays a histogram with the length of each bar to each estimated effect as shown in figure(20). From the Pareto chart it can be also noted that there are five significant parameters at a 90% confidence level: the inlet velocity A, swirl angle B, and the combinations AA, BB, and AB. Pareto chart also shows all linear and second-order effect of the variables within the model and estimates the significant of each with respect to maximizing the pressure drop response at 90% confident level.

### 4.3.5 Multiple Response Optimization

Harrington proposed a desirability function which is the most strongly and popular suggested method for multiple response optimization problems [21]. Table 6 shows the desirability function evaluated at each point in the design that optimize value of inlet parameters. Among the design points, it is clear that the maximum desirability is achieved at run 7.

		<i>Predicted</i>	<i>Observed</i>
<i>Row</i>	<i>Pressure Drop</i>	<i>Desirability</i>	<i>Desirability</i>
1	246.0	0.100129	0.0400467
2	649.9	0.141732	0.130764
3	67.7	0.0	0.0
4	1340.0	0.248969	0.285762
5	2940.0	0.694676	0.645127
6	224.0	0.00567808	0.0351055
7	4520.0	0.956673	1.0
8	1770.0	0.437102	0.382342
9	1876.0	0.362999	0.40615

Table 7 Multiple response optimization using desirability function

<i>Factor</i>	<i>Low</i>	<i>High</i>	<i>Optimum</i>
Inlet Velocity	0.75	4.75	4.75
Swirl Angle	14.17	80.83	39.5693

Table 8 Optimization input parameters

Table 8 clearly showed that the pressure drop reach its minimize as the inlet velocity and swirl angle falls into range of 4.75m/s and 39.569°, respectively, and the optimum pressure drop is achieved at **88 Pa**.

## **CHAPTER 5**

### **5.0 CONCLUSION AND RECOMMENDATION**

The present project implied the use of CFD simulation to study the flow characteristics of swirling flow in a single phase in inline separator. Although the separator will be used for multi-phases, it is useful first to analyze single phase flow since single phase flow is computationally less expensive ,less complex than multiphase , making it easier to study the flow behavior in parameter studies. In this project, Nine models has been designed with different swirl angles and inlet velocities using Ansys 15.0

From the result obtained in the simulation, the pressure drop observed in the internal surface element is the largest when the inlet velocity is high which leads to a large pressure drop necessary to generate the swirl flowing. Also, it can be noted from the results, an internal surface element with different swirl angles will lead changing the downstream velocity distribution and will therefore alter the flow behavior. This shows a smaller annular reversed flow region is formed for lower swirl angles which can lead to improve the separation efficiency. Finally, Response surface methodology was used to obtain the minimum pressure drop in inline separator and it showed that a change in swirl angle leads a small change in pressure drop compare to the inlet velocity. that has more effect than swirl angle.

There are some recommendations in order to improve this study;

- Further studies can be conducted for two phases flow in inline separator.
- Additional studies can be run on the effects of flow rates, temperature and geometry dimensions.

## REFERENCES

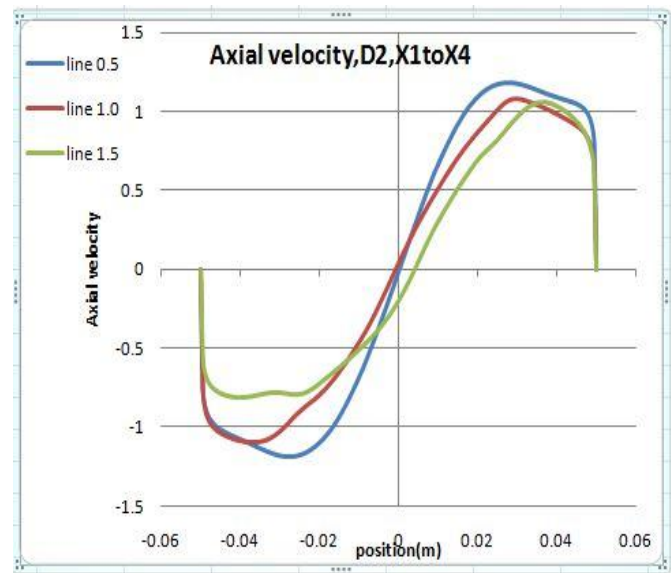
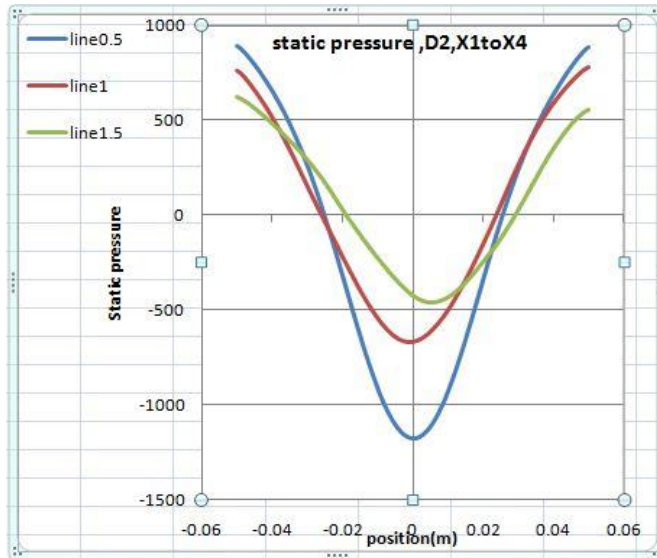
- [1] Y.Liu,F.J.Zhou,Y.C.Zhang,et al,”A practice of polymer flooding during middle-high water cut in Bohai oilfields,China Offshore oil and Gas”,24,1,2012,pp.93-96
- [2] Peachy, B.R., Solanki, S., Zahacy, T., and Piers, K.D.: “Downhole Oil/Water Separation Moves into High Gear”, 1997 Petroleum Society of CIM Annual Technical Meeting, Calgary, Jun. 11.
- [3] A. C. Hoffmann and L. E. Stein. Gas cyclones and swirl tubes: Principle, Design and Operation. Springer, 2nd edition, 2008.
- [4] BELT, R. (2007). On the liquid film in inclined annular flow. Ph.D. thesis, Delft University of Technology. BRADLEY, D. (1965). The Hydrocyclone. Pergamon Press.
- [5] Slot, J.J.; Campen, van L.J.A.M.; Hoeijmakers, H.W.M.; Mudde, R.F. IN-LINE OIL-WATER SEPARATION IN SWIRLING FLOW, (2011).
- [6] DIRKZWAGER, M. (1996). A New Axial Cyclone Design for Fluid-Fluid Separation. Ph.D. thesis, Delft University of Technology.
- [7] HANJALIC, K. (1999). “Second-Moment Turbulence Closures for CFD: Needs and Prospects”. International Journal of Computational Fluid Dynamics, 12(1), 67–97.
- [8] MURPHY, S. et al. (2007). “Prediction of strongly swirling flow within an axial hydrocyclone using two commercial CFD codes”. Chemical engineering science, 62, 1619–1635.
- [9] R. Delfos, S. Murphy, D. Stanbridge, Z. Olujic, and P.J. Jansens. A design tool for optimising axial liquid-liquid hydrocyclones. Minerals Engineering, 17(5):721–731, 2004.
- [10] KO, J. (2005). Numerical modelling of highly swirling flows in a cylindrical through-flow hydrocyclone. Ph.D. thesis, Royal Institute of Technology.
- [11] KHAROUA, N. et al. (2010). “Hydrocyclones for de-oiling applications-a review”. Petroleum Science and Technology, 28, 738–755.
- [12] A.K. Gupta, D.G. Lilley, N. Syred, Swirl Flows, Abacus, Tunbridge Wells, Kent and Cambridge, Mass, 1984, pp. 13–117.
- [13] O. Kitoh. Experimental study of turbulent swirling flow in a straight pipe. Journal of Fluid Mechanics, 225:445–479, 1991.
- [14] C. Gomez, J. Caldentey, and S. Wang, L. Gomez, R. Mohan, and O. Shoham, “Oil/Water Separation in Liquid/Liquid Hydrocyclones (LLHC): Part 1 – Experimental Investigation”, SPE J., pp. 353–361, (2002).
- [15] A.K. Gupta, D.G. Lilley, N. Syred, Swirl Flows, Abacus, Tunbridge Wells, Kent and Cambridge, Mass, 1984, pp. 25–
- [16] M. Ishii and M. Zuber. Drag coefficient and relative velocity in bubbly, droplet or particulate flows. AIChE Journal, 25, 1979.
- [16] J. Caldentey, C. Gomez, S. Wang, and L. Gomez, R. Mohan, and O. Shoham, “Oil/Water Separation in Liquid/Liquid Hydrocyclones (LLHC): Part 2 – Mechanistic Modeling”, SPE J., pp. 362–372, (2002)

- [17]DIRKZWAGER, M. (1996). A New Axial Cyclone Design for Fluid-Fluid Separation. Ph.D. thesis, Delft University of Technology.
- [18]E. C. Jr. Harrington. The desirability function. *Industrial Quality Control*, 21:494–498, 1965.
- [19]G. E. P. Box and K. B. Wilson. On the experimental attainment of optimum conditions. *Journal of the Royal Statistical Society*, 13:1– 45, 1951.
- [20]F. Boysan, W.H. Ayer, and J. A. Swithenbank. Fundamental mathematical-modelling approach to cyclone design. *Transaction of Institute Chemical Engineers*, 60:222–230, 1982.
- [21]E. .C.Jr. Harrington. The desirability function. *Industrial Quality Control*, 21:490–498, 1965.

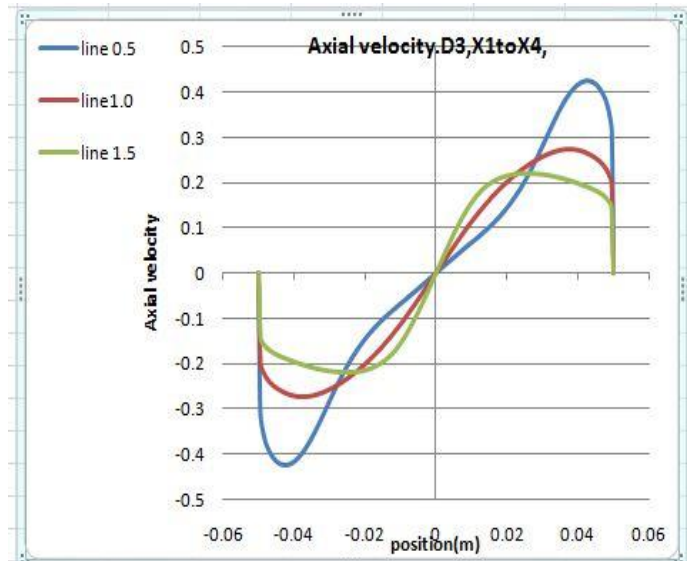
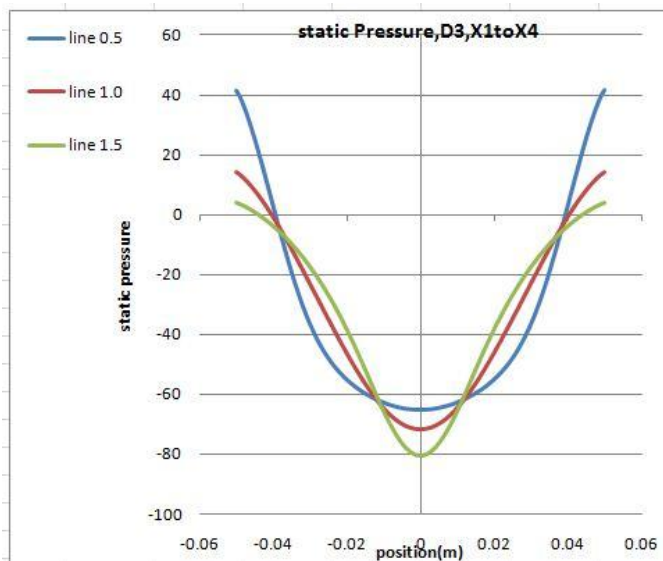
## Appendixes

Radial distribution of static pressure and inlet velocity on the line through center of pipe at  $x=0.5, 1.0, 1.5$  for model 2, 3, 4, 5, 6, 7, and 8.

### Model 2

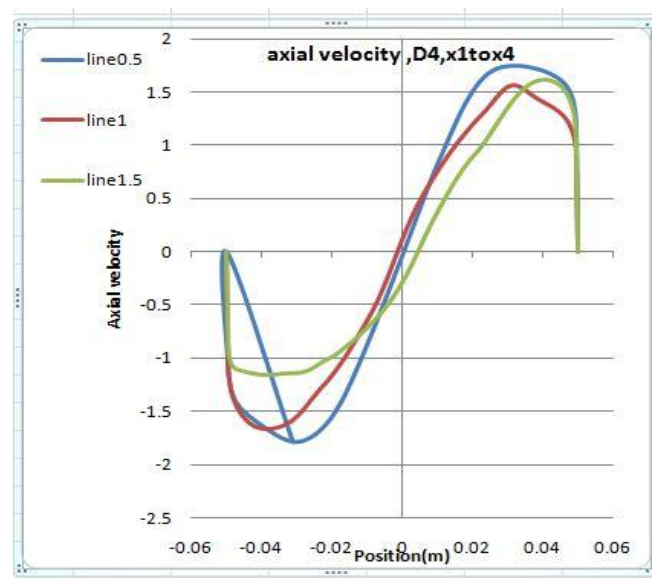
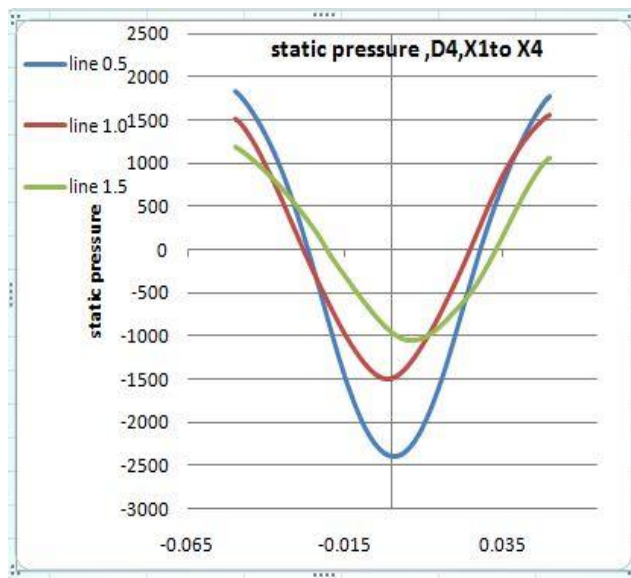


### Model 3

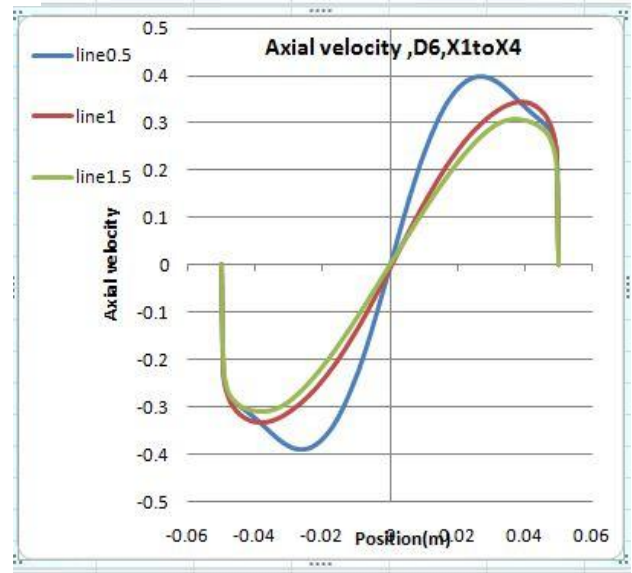
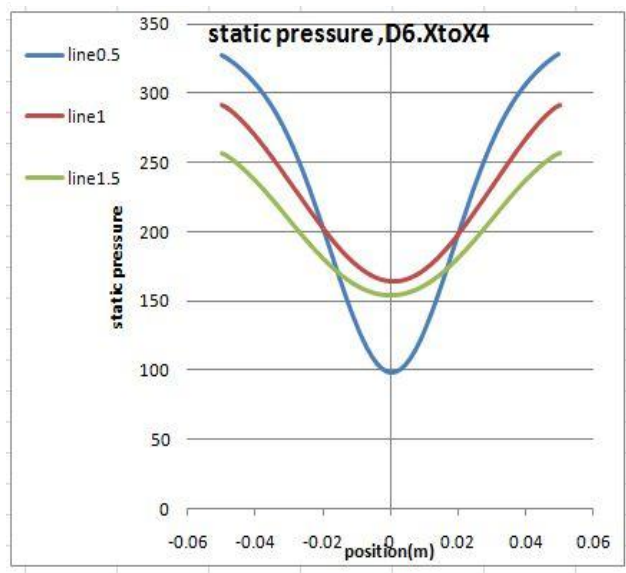




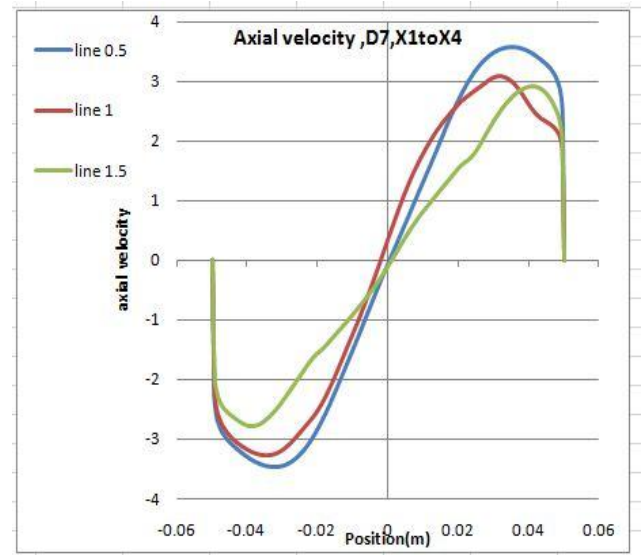
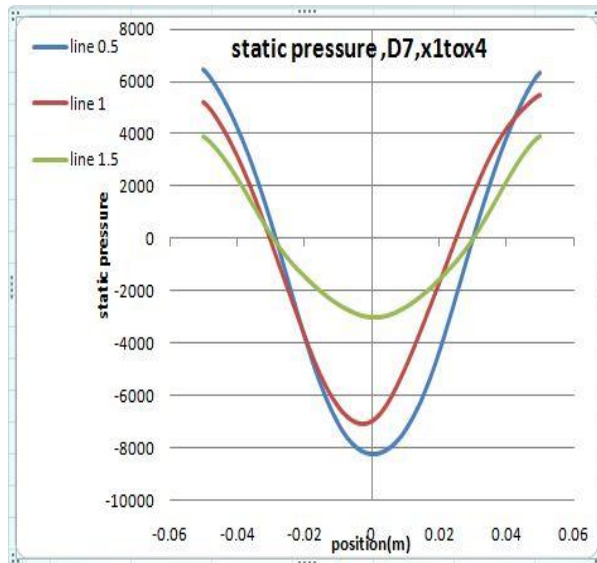
## Model4



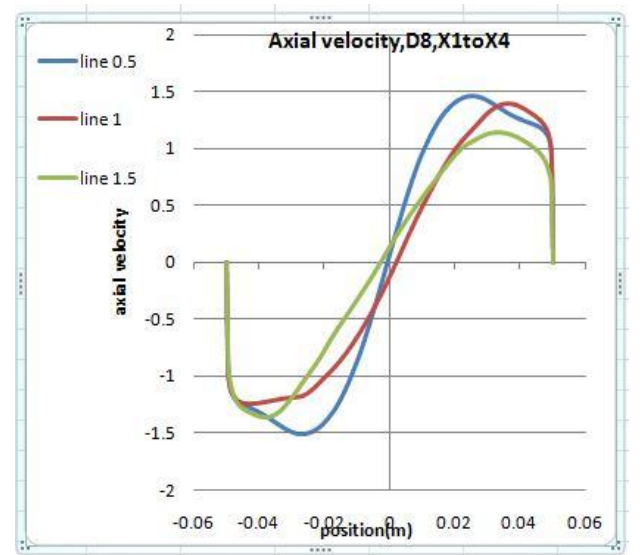
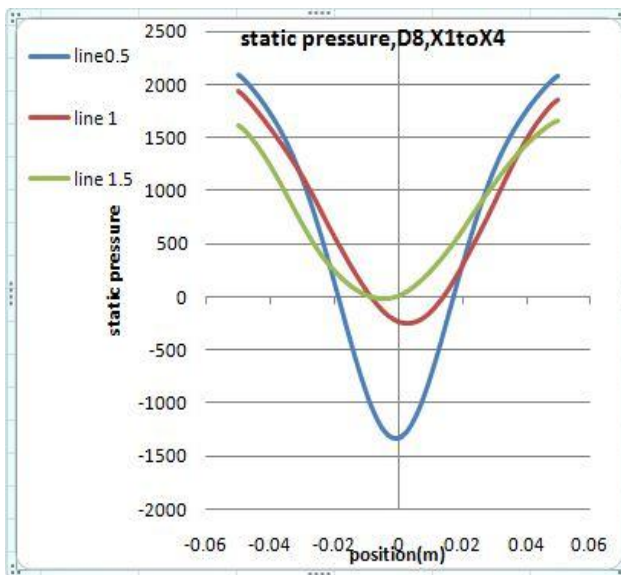
## Model 5



## Model6



## Model7



## Model8

